Kinetics of silicide formation over a wide range of heating rates spanning six orders of magnitude

Manel Molina-Ruiz, Aitor F. Lopeandía, Marta Gonzalez-Silveira, Gemma Garcia, Inma Peral, Maria T. Clavaguera-Mora, and Javier Rodríguez-Viejo

---

Kinetics of silicide formation over a wide range of heating rates spanning six orders of magnitude

Manel Molina-Ruiz,[1] Aitor F. Lopeandía,[1] Marta Gonzalez-Silveira,[1] Gemma Garcia,[1] Inma Peral,[2] Maria T. Clavaguera-Mora,[1] and Javier Rodríguez-Viejo[1,3,a)]

[1]*Grup de Nanomaterials i Microsistemes, Departament de Física, Universitat Autònoma de Barcelona, 08193 Bellaterra, Spain*
[2]*ALBA Synchrotron Light Facility, 08290 Cerdanyola del Vallès, Spain*
[3]*MATGAS Research Centre, UAB Campus, 08193 Bellaterra, Spain*

Kinetic processes involving intermediate phase formation are often assumed to follow an Arrhenius temperature dependence. This behavior is usually inferred from limited data over narrow temperature intervals, where the exponential dependence is generally fully satisfied. However, direct evidence over wide temperature intervals is experimentally challenging and data are scarce. Here, we report a study of silicide formation between a 12 nm film of palladium and 15 nm of amorphous silicon in a wide range of heating rates, spanning six orders of magnitude, from 0.1 to 10^5 K/s, or equivalently more than 300 K of variation in reaction temperature. The calorimetric traces exhibit several distinct exothermic events related to interdiffusion, nucleation of Pd_2Si, crystallization of amorphous silicon, and vertical growth of Pd_2Si. Interestingly, the thickness of the initial nucleation layer depends on the heating rate revealing enhanced mass diffusion at the fastest heating rates during the initial stages of the reaction. In spite of this, the formation of the silicide strictly follows an Arrhenius temperature dependence over the whole temperature interval explored. A kinetic model is used to fit the calorimetric data over the complete heating rate range. Calorimetry is complemented by structural analysis through transmission electron microscopy and both standard and *in-situ* synchrotron X-ray diffraction. © 2014 AIP Publishing LLC. [http://dx.doi.org/10.1063/1.4890106]

Solid-state reactions between two thin film materials are central to many applications in relevant areas such as electronics, materials science, and surface science. An example with important implications in nowadays microelectronic industry is the reaction between an ultrathin metal layer and silicon to form low-resistive materials to be used as metal gates. NiSi,[1–3] or more recently Ni(Pt)Si,[4] are the silicides of choice for actual sub-nm devices. The kinetics and thermodynamics of formation of those silicides are often complex due to the creation of intermediate metastable phases before the stable one sets in. For instance, NiSi formation starting from 13 nm Ni on single-crystalline Si is preceded by a mixture of Ni_2Si and Ni_3Si_2 phases.[5] In the present study, we focus our analysis on the reaction between Pd and Si, since only one stable phase forms below 800 °C.[6–8] Overall mechanisms of silicide formation: diffusion plus reaction, and their activation energies are relatively well described in isothermal annealings or moderate temperature up scans for a variety of silicides. However, the dependence on ramp rate is not at the same level of maturity and further investigations are required. The continuous decrease of the dimensions of electronic devices imposes stringent processing conditions to minimize interdiffusion and cross-talk effects between the different regions of the device. Fast heating processes are thus being considered to reduce the adverse impact of more traditional long-thermal treatments.[9,10] In most studies involving thermodynamic or structural parameters, the heating rate achievable is limited by the experimental technique,

i.e., by the temporal resolution to obtain accurate data. Traditional heating rates in calorimetric studies are below 10 K/s. Only very recently nanocalorimetry has been used to analyze silicide reactions at ultrafast heating rates.[11–13] Needless is to say that it is experimentally challenging to measure intermediate reactions between ultrathin layers of various elements in a very wide heating rate range. In this paper, we circumvent this difficulty by using a combination of calorimetric techniques, from standard differential scanning calorimetry (DSC) to fast-scanning nanocalorimetry, to evaluate the kinetic and thermodynamic parameters that control the formation of Pd_2Si from the reaction between ultrathin layers of palladium (Pd) and amorphous silicon (a-Si) by changing the heating rate by six orders of magnitude. We complement our data by *in-situ* synchrotron radiation analysis of phase formation and structural analysis by transmission electron microscopy.

Thin films of a-Si (15 nm thick) and Pd (12 nm thick) were sequentially grown on aluminum (Al) foil or onto the SiN_X membrane of a calorimetric chip by electron beam evaporation from targets of pure Si 99.999% and Pd 99.95%. The Al foil was previously covered by a thin SiO_2 layer to prevent interaction with the a-Si layer during heat treatments in the DSC. The foil is then folded and introduced in the DSC pan, allowing a net mass of Pd/a-Si of ∼0.1 mg. Given the initial thickness of the Pd and a-Si layers, the expected product of the reaction should be ∼20 nm of Pd_2Si, with a slight excess of Si after the reaction is completed. Since a single instrument can hardly analyze the transformation of ultrathin films in the very large heating rate interval proposed here

(from 0.1 to 10^5 K/s), we use two different setups and three methodologies to obtain accurate power vs. temperature data during the silicide formation. At slow heating rates, 0.1 and 1 K/s, the calorimetric scans were recorded with a differential scanning calorimeter (Perkin Elmer DSC 7), while for $10–10^5$ K/s the measurements were done using membrane-based nanocalorimeters. In particular, at rates above 2×10^4 K/s, we use quasi-adiabatic nanocalorimetry (QAnC).[14,15] In this last technique, a constant current pulse heats the sample at ultrafast rates and the measurement of the voltage variation of the calorimetric transducer permits to infer the heat capacity. Since the heat involved in the reaction between ultrathin layers is very small, we work in differential mode, i.e., two chips (sample and reference) are used in the measurements. To obtain the heat capacity, we subtract the contribution of the addenda, previously evaluated by multiple scans on empty nanocalorimeters. We also correct for small heat losses by carrying out measurements at various heating rates. The noise in the heat capacity at 300 K is ~50 pJ/K. In the intermediate heating rate regime, $10–10^4$ K/s, the quasi-linear increase in temperature is achieved using saw-tooth nanocalorimetry (STnC) current-time profiles.[16] In this range, heat losses are important, and we only access an apparent heat capacity. A second up scan was always performed for baseline correction. The temperature calibration of the nanocalorimeters was verified on every device after silicide formation by measuring the melting point of Sn and Al layers. Those films were grown on top of the Pd_2Si layer after capping it by a 30 nm thick SiO_2 insulating film. Cross sectional transmission electron microscopy (XTEM, Jeol JEM-2011 at 200 kV) and XRD (Philips X'Pert, Cu Kα source at $\lambda = 1.5418$ Å) were used to characterize the product of the transformation after various thermal treatments. For standard X-ray characterization multilayers consisting of 10 periods of 12 nm Pd + 15 nm Si + 30 nm SiO_2 were grown. *In-situ* XRD measurements were carried out at the MSPD beamline[17,18] of the ALBA Synchrotron Light Facility at Barcelona directly onto calorimetric chips.

In Figure 1, we show the calorimetric measurements covering the heating rate interval from 0.1 to 10^5 K/s. The curves are normalized to their maximum intensity for the sake of clarity [Figures 1(a) and 1(b)]. The calorimetric traces show two broad exothermic features which shift towards higher temperatures as the heating rate increases. Only in the curve obtained at 10 K/s, using STnC [Figure 1(b)], the first exothermic jump is not resolved. This is the result of the lower sensitivity at these low heating rates. An extensive structural and calorimetric study reveals that the two broad exothermic jumps, observed in Figure 1, are composed of four calorimetric peaks associated to different mechanisms of transformation, producing most likely a single phase, Pd_2Si [see supplementary material for further information on the nature and microstructure of the phases].[19] The nature of the low temperature broad change on heat capacity is inferred by analyzing the influence of several mild heat treatments to the calorimetric signal. These measurements confirm that the first exothermic jump corresponds to intermixing of Pd and a-Si to build up an amorphous/nanocrystalline layer at the interface followed by nucleation of Pd_2Si along the Pd/a-Si interface. This is in
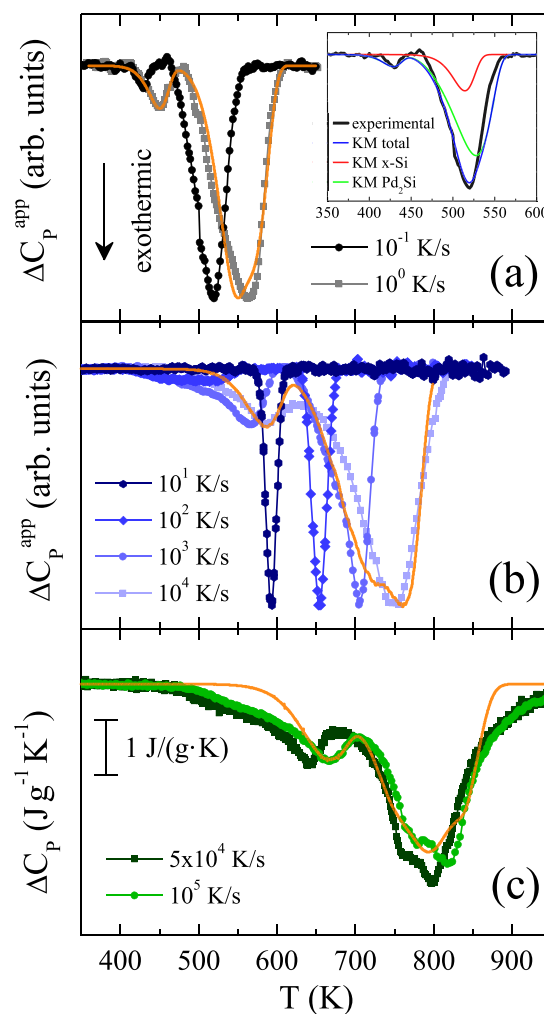
FIG. 1. Calorimetric data of the silicide reaction. Apparent heat capacity vs. temperature measured with: (a) DSC at 0.1 and 1 K/s and (b) STnC methodology at intermediate heating rates from 10 to 10^4 K/s. (c) Specific heat as a function of temperature obtained at 5×10^4 and 10^5 K/s. The solid orange lines correspond to the calculated data using the KJMAE formalism. The inset in (a) shows the experimental data for the sample measured at 0.1 K/s and the fitting curves obtained from the KM showing the Pd_2Si formation (green line) and the a-Si crystallization (red line).

agreement to a significant number of previous reports that attribute the presence of the first feature to nucleation barriers that control the initial phase formation.[20] The second broad exothermic jump corresponds to both the a-Si crystallization (x-Si) and the vertical growth of the Pd_2Si phase [see supplementary material and Figure 1(a), inset]. In fact, the large enthalpy associated with the DSC and QAnC calorimetric traces [Figures 1(a) and 1(c)] with respect to pure Pd_2Si formation clearly indicates other processes are active in this temperature range. The enthalpy of the complete reaction at the fastest rates is 93 μJ, which includes 18 μJ due to intermixing at the interface, 12 μJ as a result of the crystallization of 11 nm (~26 ng) of a-Si,[13] and 63 μJ due to the formation of 180 ng of Pd_2Si.[21]

To gain more insight into the mechanisms that control the phase transformation in the whole temperature interval, we use the Kolmogorov–Johnson–Mehl–Avrami–Erofeev (KJMAE) formalism to fit the calorimetric traces.[22,23] For the sake of clarity, we only include fitting curves for the highest heating rate of every measurement technique (solid

orange lines in Figure 1). The complete set of fittings and the equations used to describe the main processes are described in detail in supplementary material.[19] The kinetic model (KM) incorporates the following processes: (i) nucleation of Pd_2Si within the Pd_xSi_{1-x} interfacial region, (ii) a-Si crystallization through a growth front from the interface, and (iii) vertical growth of Pd_2Si. Note that the kinetic model does not include the intermixing reaction. The crystallization of a-Si is catalyzed by the presence of the Pd_2Si phase and therefore occurs at lower temperatures than expected for pure Si, in agreement with many previous reports.[24,25] According to the kinetic model, the crystallization of a-Si and the vertical growth of Pd_2Si are fully overlapped [inset of Figure 1(a) and supplementary material].

The analysis and interpretation of the temperature evolution of those exothermic events is the main outcome of the present work. The general trend can be rapidly appreciated from Figure 1. As the heating rate is increased up to 10^5 K/s, the onset and maximum of the peaks shift to higher temperatures as expected for thermally activated processes. To obtain a first insight, we use a simplified methodology, the Kissinger plot (Figure 2), to estimate the average activation energy of the transformation during the heating ramp.[26] We consider only two main processes and average values of the heating rate, since in STnC and QAnC methodologies the heating rate is not constant throughout the measurement when silicide formation occurs.

As illustrated in Figure 2, both peaks exhibit a linear behavior in the whole temperature interval with activation energies of 1.38 ± 0.04 eV/at for the first peak and 1.75 ± 0.04 eV/at for the second one. This average energy values are slightly higher than those previously reported by Homma et al.[27] in couples of Pd/a-Si:H, where an activation energy of 1.1 eV/at for a reaction-limited Pd_2Si formation and 1.4 eV/at for a diffusion-limited growth was found. Although it is normally assumed that Pd and Si fluxes are coupled and both contribute to Pd_2Si growth, the activation energy evaluated here for the second peak coincides with the value of 1.7 eV/at found for Si mobility through polycrystalline Pd_2Si.[28]

Table I highlights the excellent agreement between the activation energies obtained for the nucleation and vertical growth of Pd_2Si using the kinetic modeling and those obtained using the Kissinger methodology. The difference between the simulated data and the experimental calorimetric traces in the low temperature region of Figure 1 highlights the increased importance of the initial interdiffusion as the heating rate increases. Interestingly, the ratio between the areas associated to the two transformation mechanisms (nucleation at the interface and vertical growth) involving Pd_2Si is not constant and shows a clear dependence with the heating rate. The variation can be easily inferred from Figure 1. The fastest is the heating rate, the higher is the proportion of Pd_2Si formed during the nucleation stage compared to the amount transformed during the vertical growth. This is reflected in the model by the parameter L_0, which indicates the initial height occupied by the Pd_2Si nuclei [Eq. (7) in supplementary material]. We identify the nucleation region with the premixed zone at the interface that has reached the required stoichiometry to initiate nuclei formation. Figure 3(a) shows the evolution of the thickness of this nucleation zone as a function of the heating rate. While at the slowest rates of 0.1–1 K/s, the nucleation process at the interface creates a 1.2 nm thick Pd_2Si layer, at fastest heating rate of 10^5 K/s the thickness of the interfacial layer grows up to 4.8 nm, four times larger.

The interfacial formation mechanism of Pd_2Si at the lowest and highest heating rates is schematized in Figure 3(b). We interpret these differences as follows: at low heating rates (0.1–1 K/s), a thin mixed disordered region forms between Pd and a-Si at temperatures below 400 K. This region acts as the seed layer for the formation of the initial nuclei of Pd_2Si that occurs around 450 K (1st calorimetric peak). On increasing the temperature, the Pd_2Si grows vertically by Pd and/or Si diffusion through the Pd_2Si interlayer. However, at ultrafast heating rates above thousands of K/s, the scheme changes dramatically. The activation energy for nucleation drives the nucleation peak towards higher temperatures ($\sim$650 K), enabling substantial intermixing before the interfacial layer has formed. As a consequence, the mixed disordered region is now four times thicker than the one obtained at slower heating rates. Since we assume nucleation only occurs within the premixed region, the heat dissipated during nucleation of Pd_2Si is also 4$\times$ larger. Remarkably, in spite of the thickness increase of the nucleation-driven interfacial Pd_2Si layer, the vertical growth strictly follows an Arrhenius temperature dependence which may indicate that the diffusion-controlled process occurs via

FIG. 2. Kissinger plot for the first (open symbols) and second (filled symbols) exothermic peaks. Data obtained from QAnC at fast heating rates (triangles), from conventional DSC at slower rates (circles), and from STnC at intermediate heating rates (squares). Continuous lines represent best fits to the data which yield the activation energies.

TABLE I. Activation energies for the Pd_2Si nucleation (E_I), Pd_2Si vertical growth (E_D), and a-Si crystallization (E_U) obtained from the kinetic model (KJMAE formalism) and experimentally (Kissinger method). L_T corresponds to the final thickness of the Pd_2Si film.

	KJMAE formalism	Kissinger method
E_I	(1.38 ± 0.05) eV/at	(1.38 ± 0.04) eV/at
E_D	(1.81 ± 0.05) eV/at	(1.75 ± 0.04) eV/at
E_U	(1.72 ± 0.05) eV/at	
L_T	(20.3 ± 2.0) nm	

(a)

(b)
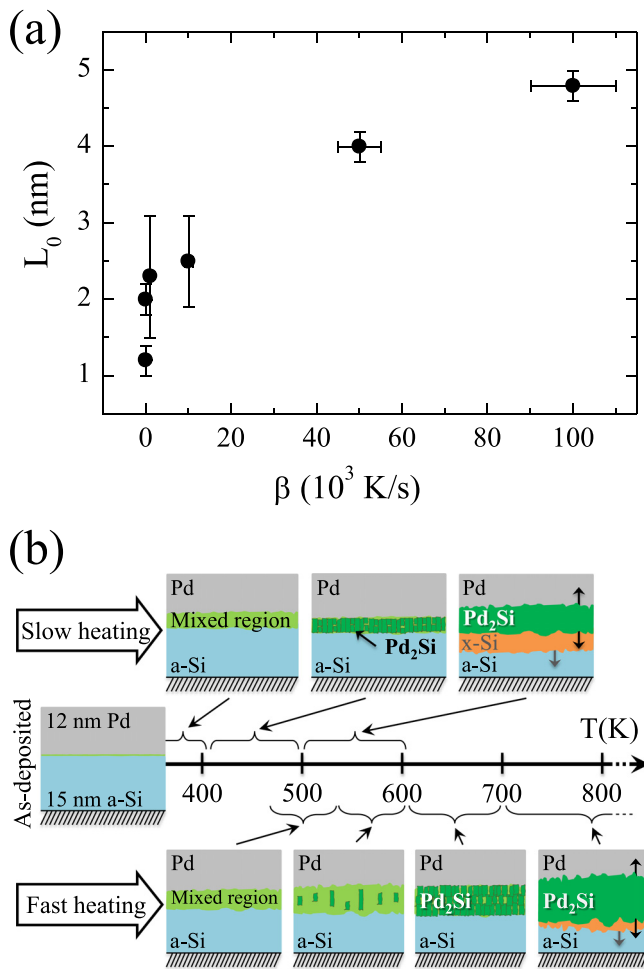
FIG. 3. (a) Thickness of the initial Pd_2Si that forms at the a-Si/Pd interface as a function of the heating rate. (b) Schematics of the initial growth mode at the interface a-Si/Pd for slow (top) and fast (bottom) heating.

fast diffusion paths, probably through grain boundaries connecting the Pd and Si reservoirs.

We have shown that the reaction of ultrathin films of Pd and a-Si is dominated by four processes: intermixing forming disordered Pd_XSi_{1-X} region at the a-Si/Pd interface, nucleation of Pd_2Si in the premixed region, crystallization of a-Si, and simultaneously vertical growth of the Pd_2Si phase. More fundamentally, when analyzed over a wide heating rate interval of six orders of magnitude, from 0.1 to 10^5 K/s, the formation of Pd_2Si, both with respect to the nucleation and the vertical growth, exhibits a pure Arrhenius behavior. The enhanced mass diffusion observed during the initial stages of the reaction increases with heating rate, due to the thermally activated nucleation of the Pd_2Si phase.

[1]P. Gas, F. M. d'Heurle, F. K. LeGoues, and S. J. La Placa, J. Appl. Phys. **59**, 3458 (1986).

[2]S. Gaudet, P. Desjardins, and C. Lavoie, J. Appl. Phys. **110**, 113524 (2011).

[3]D. Mangelinck, K. Hoummada, and I. Blum, Appl. Phys. Lett. **95**, 181902 (2009).

[4]D. Kim, A. Domenicucci, and S. S. Iyer, J. Appl. Phys. **103**, 073708 (2008).

[5]C. Rivero, P. Gergaud, M. Gailhanou, O. Thomas, B. Froment, H. Jaouen, and V. Carron, Appl. Phys. Lett. **87**, 041904 (2005).

[6]K. Hoummada, A. Portavoce, C. Perrin-Pellegrino, D. Mangelinck, and C. Bergman, Appl. Phys. Lett. **92**, 133109 (2008).

[7]M. Wittmer and K. N. Tu, Phys. Rev. B **27**, 1173 (1983).

[8]R. Suryana, O. Nakatsuka, and S. Zaima, Jpn. J. Appl. Phys., Part 1 **50**, 05EA09 (2011).

[9]H.-Y. Chen, C.-Y. Lin, M.-C. Chen, C.-C. Huang, and C.-H. Chien, J. Electrochem. Soc. **158**, H840 (2011).

[10]H.-Y. Chen, C.-Y. Lin, C.-C. Huang, and C.-H. Chien, Microelectron. Eng. **87**, 2540 (2010).

[11]L. P. Cook, R. E. Cavicchi, N. Bassim, S. Eustis, W. Wong-Ng, I. Levin, U. R. Kattner, C. E. Campbell, C. B. Montgomery, W. F. Egelhoff, and M. D. Vaudin, J. Appl. Phys. **106**, 104909 (2009).

[12]R. K. Kummamuru, L. De La Rama, L. Hu, M. D. Vaudin, M. Y. Efremov, M. L. Green, D. A. LaVan, and L. H. Allen, Appl. Phys. Lett. **95**, 181911 (2009).

[13]M. Molina-Ruiz, A. F. Lopeandía, M. González-Silveira, Y. Anahory, M. Guihard, G. Garcia, M. T. Clavaguera-Mora, F. Schiettekatte, and J. Rodríguez-Viejo, Appl. Phys. Lett. **102**, 143111 (2013).

[14]M. Y. Efremov, E. A. Olson, M. Zhang, F. Schiettekatte, Z. Zhang, and L. H. Allen, Rev. Sci. Instrum. **75**, 179 (2004).

[15]A. F. Lopeandía, J. Rodríguez-Viejo, M. Chacón, M. T. Clavaguera-Mora, and F. J. Muñoz, J. Micromech. Microeng. **16**, 965 (2006).

[16]A. F. Lopeandia, J. Valenzuela, and J. Rodríguez-Viejo, Sens. Actuators, A **143**, 256 (2008).

[17]F. Fauth, I. Peral, C. Popescu, and M. Knapp, Powder Diffr. **28**, S360 (2013).

[18]M. Knapp, I. Peral, L. Nikitina, M. Quispe, and S. Ferrer, Z. Kristallogr. Proc. **1**, 137 (2011).

[19]See supplementary material at http://dx.doi.org/10.1063/1.4890106 for more details on calorimetric traces and kinetic model.

[20]E. Ma, C. V. Thompson, and L. A. Clevenger, J. Appl. Phys. **69**, 2211 (1991).

[21]J. C. C. Fan and C. H. Anderson, Jr., J. Appl. Phys. **52**, 4003 (1981).

[22]K. R. Coffey, L. A. Clevenger, K. Barmak, D. A. Rudman, and C. V. Thompson, Appl. Phys. Lett. **55**, 852 (1989).

[23]M. Gonzalez-Silveira, J. Rodriguez-Viejo, G. Garcia, F. Pi, F. J. Ager, J. L. Lábár, A. Barna, M. Menyhárd, and L. Kótis, J. Appl. Phys. **100**, 113522 (2006).

[24]D. He, J. Y. Wang, and E. J. Mittemeijer, J. Appl. Phys. **97**, 093524 (2005).

[25]Z. Wang, J. Wang, L. Jeurgens, and E. Mittemeijer, Phys. Rev. Lett. **100**, 125503 (2008).

[26]H. E. Kissinger, Anal. Chem. **29**, 1702 (1957).

[27]K. Homma, T. Koike, S. Ando, K. Adachi, and M. Motohashi, Electron. Commun. Jpn., Part 2 **80**, 12 (1997).

[28]E. C. Zingu, J. W. Mayer, C. Comrie, and R. Pretorius, Phys. Rev. B **30**, 5916 (1984).